FEATURE ARTICLE

Clusters: Tools for Studying Potential Surfaces and Their Connection to Molecular Dynamics

R. Stephen Berry

Department of Chemistry, The University of Chicago, Chicago, Illinois 60637

Received: January 13, 1994; In Final Form: April 26, 1994®

Clusters provide a particularly convenient laboratory for studying general characteristics of multidimensional potential surfaces and for relating the forms of those surfaces to the dynamics exhibited by the objects whose properties are governed by these surfaces. The multidimensional potentials of systems such as atomic van der Waals clusters and the binary clusters of alkali halide molecules can be represented very reliably, and now molecular van der Waals clusters of such species as CCl_4 can be represented with considerable confidence as well. The extent of validity has been established for classical mechanical simulations, so that credence can now be given to the results of classical molecular dynamics simulations of clusters of second-row and heavier species. These illustrate finite-system counterparts of various kinds of phase changes, isomerization, and evolution of chaotic and ergodic behavior, as well as the effects on multidimensional potential surfaces of the character of the forces between pairs of particles.

I. Introduction

Many chemical processes conform conveniently to our adiabatic, Born–Oppenheimer model in which motion of the system's atoms takes place on a single potential surface. The surface has high dimensionality, in general—$3N-6$ for a nonlinear system consisting of N atoms—and in most cases has many, many minima. Even cases that require us to include surface crossings are often amenable to treatments that start with the system on a single, multidimensional effective potential surface, however complicated. If we know a surface, we can, at least in principle, describe the behavior of our system on that surface, for example by using classical mechanics in molecular dynamics simulations or by propagating quantum-mechanical wave packets.

The obstacles to applying these notions have been several. First, for molecules of more than three or four atoms, it has been exceedingly difficult to determine effective potentials extensively enough to make them useful for anything more than describing the vicinity of known, stable structures. The second confronts us when we ask what significant information we want regarding the form of the surface; this information invariably includes some catalogue of the minima and of the saddles that connect them and may include more, such as the amount of configuration space or phase space available to the system, the topology of the surface, and the curvatures, at least in the vicinity of the saddles and the minima. Until recently, only the minima could be found easily and reliably; now, at least we can include the saddles in this list of accessible information. A third obstacle arises if we try to deal with systems of more than six or eight or ten atoms: the number of minima and the complexity of the effective potential surface grow so rapidly with the number of atoms in the system that we do not want to know the energies and geometries of the system in all the local minima in the surface, to say nothing of the energies and geometries of the saddles that connect those minima. We need some way to describe their distributions in a statistical, summarizing manner. Fourth, and this applies specifically to quantum-mechanical distributions, it has been difficult and very expensive to carry out propagation of wave packets in many-dimensional spaces, although it is now feasible in two dimensions.[1,2]

The first three of these problems will concern us heavily here; the fourth will be of much less concern because Doll and coworkers have shown that, for describing the kinds of phenomena we consider here, quantum characteristics are very important even qualitatively for aggregates of helium and other species of comparable mass, are quantitatively nonnegligible for accurate treatments of systems comprised of species as massive as neon, and are of only very small importance for systems made of atoms with masses in the range of argon or larger.[3-5] We shall restrict our discussion primarily to systems and conditions for which classical mechanics is fairly reliable. This removes the fourth obstacle.

The first obstacle remains if we insist on describing processes in conventional molecules. However, we can sidestep that difficulty if we use as our model systems certain kinds of clusters instead of molecules. This is not because we are unconcerned about molecules, not at all. It is because we know enough now to say a great deal about the sensitivity of many properties of polyatomic systems to details of the potential and therefore, with care, can use systems with simple potentials to tell us about some systems with complicated potentials. Clusters or molecules whose component particles are atoms, whose dominant interactions are isotropic pair interactions, differ from each other if the *ranges* of their potentials differ, but are very similar if their potentials have similar ranges and curvatures at their minima, even if the analytic forms of those potentials are quite different. On the other hand, clusters in which anisotropies dominate the interparticle forces at moderately long ranges and in the vicinity of their potential minima—molecular clusters in particular—have properties quite different from those of atomic clusters, particularly structural properties.[6-8]

This means that clusters of particles reliably described by known pair potentials or other general interparticle potentials are ideal systems with which to explore multidimensional potential surfaces and the dynamics on those surfaces. We can indeed use simple models to give us reliable information about complicated systems. The best examples of such simple models are of course rare gas clusters, particularly Ar, Kr, and Xe, for which quantum corrections are negligible for most purposes, and alkali halide clusters, followed by van der Waals clusters of molecules such as CCl_4. The rare gas clusters are usually treated for modeling

® Abstract published in *Advance ACS Abstracts*, June 1, 1994.

0022-3654/94/2098-6910$04.50/0

purposes with Lennard-Jones interparticle pair potentials of the form $V(R_{ij}) = A_{ij}(R_{ij}^{-12} - R_{ij}^{-6})$, but more elaborate potentials have been used, even the elaborate potentials of Aziz et al.,[9-12] with relatively little quantitative change in the dynamics. Inclusion of polarization terms that give angle-dependent effective interactions, such as Axilrod–Teller terms, also makes only a small, quantitative change in the dynamics.[13]

Furthermore, replacing pairwise Lennard–Jones potentials with pairwise Morse potentials of the same well depth and the same second derivative at the minima leaves the general features of the multidimensional potential surface almost unchanged. However, changing the ranges and curvatures at the minima has strong effects on the shape of the multidimensional surface, which will be discussed below. Turning again to binary clusters, we find that alkali halide clusters are most frequently represented with a Born–Mayer potential, an exponential short-range repulsion between ions and a Coulombic long-range interaction, attractive for oppositely charged ions and repulsive for pairs of ions of like charge. More accurate pair potentials and inclusion of polarizabilities make small quantitative changes but do not affect the structure of the potential surface in any qualitative way.[14,15]

Exploring Multidimensional Surfaces

At present, it is rather straightforward to search for minima and saddles on surfaces of moderately high dimensionality, e.g., the 159-dimensional surface of Ar_{55}. For a cluster of 6 or 8 or even 10 atoms, ions, or molecules, we can expect to find all the minima and most important saddles connecting these minima. Hoare and Pal carried out extensive searches to determine as complete catalogues as possible of the locally stable geometries of clusters bound by Lennard-Jones and then Morse pairwise forces.[16-18] Their searches were based, for the most part, on establishing growth sequences, successive addition of one new particle, say the Nth, to each stable, available site on each stable structure. This procedure yields most but not necessarily all of the stable structures of the N-particle cluster. If one is trying to be exhaustive, it is important to supplement the growth sequence search with random searches that rely on molecular dynamics (or Monte Carlo methods) with sporadic quenches;[19-21] only in this way can one find structures that begin new growth sequences at moderately large values of N. From a knowledge of each structure and how they are linked by saddles on the potential surface $^{q}V(\mathbf{R})$, we may hope to construct and predict the high-resolution, rotation–vibration spectra of such clusters. We know, for example, that clusters of atoms held together primarily by central, pairwise forces tend to have geometries based on icosahedra, in some systems even up to clusters of several thousand atoms. The closed-shell, complete icosahedra described by Mackay[22] are especially stable; the first few of these contain 13, 55, 147, 309, 561, and 923 atoms and can be identified in mass spectra.[23] Many of the clusters of sizes between these "magic numbers" have structures that can be grown from the closed-shell icosahedra; the 19-atom cluster of argon has a doubled icosahedral structure, for example.

Another class of clusters that lend themselves to the study of potential surfaces and the dynamics on them is the alkali halides.[24-34] The interactions of the components of these clusters can be well treated with Born–Mayer potentials, i.e., sums of Coulomb attractions or repulsions to represent the long-range interactions and exponential repulsive potentials to represent the short-range interactions.[27] In contrast to the rare gas clusters and other homogeneous clusters primarily bound by central, pairwise interactions, alkali halide clusters composed of more than about three molecules tend to have rocksalt-like structures as their most stable forms.

Clusters of metal atoms also exhibit stable, "magic number" sizes, but at least for simple metals up to sizes of hundreds of atoms, these especially prominent clusters are characteristic of the electronic structure, not of the atomic packing.[35] Sodium clusters show especially prominent peaks in mass spectra at N = 8, 20, 40, and 58,[36] corresponding to the closed-shell structures of fermions in a sphere.[37] This makes the potential surfaces of metal clusters rather more complicated to study than those of rare gases or alkali halides.[38]

TABLE 1: Number of Geometrically Different Minima for Several Kinds and Sizes of Small Clusters. Homogeneous Clusters with Lennard-Jones and Morse Potentials; Alkali Halide Clusters, Based on Born–Mayer Potentials

potential	no. of particles	no. of kinds of minima
Lennard-Jones[a]	6	2
	7	4
	8	8
	9	18
	10	57
	11	145
	12	366
	13	988
Morse[b]	6	3
	7	5
	8	8
	9	16
	10	24
	11	12
potential	**no. of MX pairs**	**no. of kinds of minima**
Born-Mayer[c]	4	7
	5	13

[a] Taken from ref 16. [b] Taken from refs 16 and 58. The number of minima depends on the range of the Morse pair potential, as shown in ref 58. [c] Taken from ref 20; several but by no means all the locally stable geometries of $(MX)_n$ clusters, $2 \leq n \leq 12$, are given in ref 21.

Despite our capacity to search out the stable structures, it is out of the question to try to find all the minima on the potential surface $^{q}V(\mathbf{R})$ of a cluster containing, say, 30 or more particles, to say nothing of finding its saddles; there are simply too many. The numbers of geometrically inequivalent minima known for the potential surfaces of several species are shown in Table 1. This number increases approximately exponentially with N, the number of particles in the cluster. Furthermore, the number of permutational isomers of each of these is roughly $N!$ for homogeneous clusters and $[(N/2)!]^2$ for binary clusters such as alkali halides. The number is higher for molecular clusters because of any minima that have symmetry-based rotational isomers. In short, the number of minima and of isomeric structures increases so fast with N that we want to avoid using the vast body of information we have the computational power to generate.

Nevertheless, we do want information about the local minima and the saddles that connect them. The methods are now fairly well established. To find minima, the method of steepest descents[20,21] seems most obvious, but the related, conjugate gradient method is usually much faster.[39] Computational algorithms are readily available for both,[40] but new and more powerful methods continue to be developed.[41-44]

Two ways have emerged for finding saddles: a faster, "hill-climbing" method[45-52] and a "skiing-down" method that assures one will find important saddles, the method called "slowest slides".[53-56]

The former method starts from a chosen local minimum and a chosen normal mode of vibration at that minimum; one follows that mode up the potential surface, readjusting along the way for changes in the local curvature so that the uphill path follows the same, continuously-varying eigenvalue and eigenvector of the Hessian matrix of the potential. This process will inevitably bring the path to a saddle or to a bifurcation whose branches must lead to saddles or to further bifurcations, until eventually all branches reach saddles. This procedure is between about 3 and 8 times faster than the method of "slowest slides" but does not always find the saddles that are most frequently visited. To assure this,

it is useful to use a method that selects the saddles to be located on the basis that trajectories do cross them, especially if they cross them fairly frequently. The method of slowest slides does this. One lets a molecular dynamics simulation tell when a trajectory has gone over a maximum (along that path) in potential energy. Starting the cluster now at a configuration near that where the maximum is passed, one removes all the kinetic energy from ("quenches") the cluster[57] and then determines a downward trajectory according to the equation for steepest descent, $d\mathbf{R}/dt = -\nabla\mathcal{V}(\mathbf{R})$, where dt is replaced by the elementary step unit of the simulation and the gradient and $\mathbf{R}$ refer to the full space of all the vibrational coordinates. When this method is used to find a minimum, the coordinates virtually stop changing when the path has come very close to that minimum. When the method is used to locate a saddle, the rate of descent slows as the saddle is approached but is not exactly reached and then speeds up as the trajectory veers off and starts down toward a local minimum. The point at which the rate of descent is a minimum is taken to be the point closest, on that trajectory, to the saddle. One or two iterations then suffice to locate the saddle sufficiently accurately for any purpose we have yet found. When the minima and saddles have been located, one can get some insight by constructing a schematic cross section of the potential surface such as those shown in Figure 1 for two quite different kinds of clusters, the Ar_7 cluster[58] and the $(KCl)_4$ cluster.[30]

When one knows the geometry of a system at a saddle, one can determine the entire "reaction path" or path of least energy between the two minima connected by that saddle, simply by applying either of the methods for locating minima, starting with points near the saddle of interest. It is then straightforward to use computer graphics to display animations of reactions along reaction paths and to compare these with animations of clusters following the paths taken in full molecular dynamics simulations, either at constant energy or at constant temperature. In general, of course, the trajectories found by solving equations of motion are far off the "bull's-eye" of the "reaction path", even though they do get across the saddle. This is especially so for clusters of five or more particles; one can see some connection between classical, mechanical trajectories and the reaction path trajectory in systems of three and even four particles.

One of the foremost outstanding problems now is the evaluation of the microcanonical entropy, essentially the logarithm of the hyperarea available to a cluster of fixed energy, the size of the connected region containing the initial configuration of the system, so long as we can assume that the system is ergodic, i.e., will come arbitrarily close to every point in that connected region. This is equivalent to asking for the area of a lake in a $(3N-6)$-dimensional space. More specifically, in practice it amounts to asking for an estimate of that area from a knowledge of the locations of some small number of points on its periphery. This can be done, in principle, by three, successively more accurate methods: the spherical shell, applied recently to estimating volume of clusters,[59] the convex hull method,[60,61] and the α-shape method.[62] None has yet been used; in fact, the α-shape method has yet to be put in algorithmic form for dimensionality higher than 3. Rather, harmonic approximations have been used to describe potential wells as paraboloids,[63] from which densities of states can be computed; sometimes these have been supplemented with anharmonic corrections.[64] Probably the best methods to date for estimating the microcanonical entropy use Monte Carlo sampling to construct histograms from which the densities of states are estimated.[65,66] Variants of this method were used to construct full phase diagrams for clusters[59] and to estimate densities of stable local minima on multidimensional surfaces.[34] Another new approach is based on adiabatic invariants: one solves the problem for a tractable case and then transforms the results adiabatically into those of the desired problem.[67]

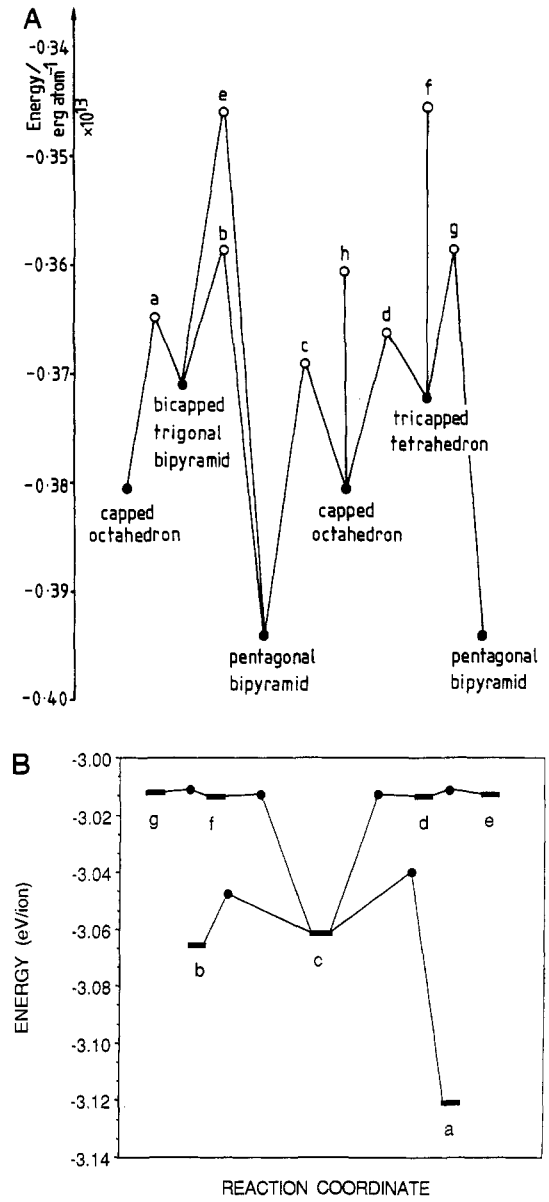

Figure 1. Schematic cross sections of potential surfaces for (A) Ar_7, with its four local minima,[58] and (B) $(KCl)_4$, with seven kinds of minima shown.[30] Minima are shown as solid circles in (A) and as short bars in (B); saddles are open circles in (A) and solid circles in (B).

Pairwise Interactions and the Shape of the Multidimensional Surface

The power and convenience of computational exploration of functions of many variables have made it feasible to find how the nature of the elementary interaction potentials between constituent particles governs the shape of their multidimensional potential surface. The most straightforward examples of this have been studies of the effect of the range of pairwise central forces on the kinds of minima and saddles the surface contains[68,69] and of the control and elimination of specific high-energy wells and barriers.[70-72] A more elaborate issue is the effect of anisotropic contributions to the shape of the surface.[13] The Lennard-Jones potential is too barren of parameters to make it useful for such studies. However, two pairwise interactions that do lend themselves to this study are the Morse potential, $V(R) = \epsilon\{\exp[2\beta(R - R_0) - 2\exp[-\beta(R - R_0)]\}$, and a generalized inverse-power potential, $V(R) = \epsilon\{[R_0/R]^{2n} - [R_0/R]^n\}$. In the Morse potential, varying β (or $\rho_0 = \beta R_0$, if $\rho = \beta R$ is used as the variable) varies the range of the pairwise interaction; in the inverse-power potential, varying the exponent n has a similar effect. We shall

refer to the simulated, homogeneous cluster of N particles interacting through pairwise Morse potentials as M_N.

The outcome of such variations[68] shows that the longer ranged is the pairwise potential, the simpler is the multidimensional potential surface $\mathcal{V}(\mathbf{R})$. If the Morse potential parameters are chosen to give the two-particle potential the same curvature at the minimum as that of the Lennard-Jones curve, the overall potential surface $\mathcal{V}(\mathbf{R})$ is essentially the same as that based on Lennard-Jones interactions. However, if the range of the pairwise Morse interaction is extended to approximately 3 times that of the Lennard-Jones 6–12 potential, then all the minima but the lowest disappear for six- and seven-particle clusters, M_6 and M_7, counterparts of Ar_6 and Ar_7. (There are two geometrically distinct minima for Ar_6 and four for Ar_7, but all the upper minima vanish when the pairwise potential has a long enough range.) In fact, each minimum for these clusters above the lowest has its own critical range, below which that minimum exists and above which it is an ordinary point on the potential surface. The behavior of the minima on $\mathcal{V}(\mathbf{R})$ [really considered as $\mathcal{V}(\mathbf{R},r_0)$] of M_7 is illustrated in Figure 2A and that of the minima and saddles for the same cluster in Figure 2B. Larger clusters show similar behavior, but low-lying minima on surfaces of large clusters need not disappear when the range of the pair-interaction potential is long but still within physically realistic limits.

Each curve above the lowest in Figure 2A terminates at its own value of ρ_0. For smaller values of ρ_0, i.e., for longer ranges of the pairwise potential, that minimum does not exist. There is, therefore, a bifurcation in the parameter space of $\mathcal{V}(\mathbf{R},\rho_0)$ at the (left) terminus of each of the curves above the lowest, at which a new maximum (saddle, in the full space) and minimum appear and persist for higher values of ρ_0; the appearance of each new minimum is accompanied by the appearance of a corresponding saddle. The energies of the minima and saddles can be mapped, as Figure 2 shows, as functions of ρ_0.

Another, more detailed kind of information also emerges from this analysis.[68] Saddles can be classified according to rank, that is, according to how many minima they connect. A rank 1 saddle has only one negative force constant or eigenvalue of its Hessian matrix, the set of second partial derivatives of the potential $\partial^2\mathcal{V}(\mathbf{R})/(\partial R_i \partial R_j)$; saddles of higher rank have successively more negative force constants or, equivalently, eigenvalues of the Hessian matrix evaluated at the saddle. Maps such as that of Figure 2B can show where a saddle changes rank, and as usually happens at such points, a new saddle of rank 1 appears as some force constant changes from positive to negative. An elegant example of this occurs in the M_6 cluster, whose lowest-energy geometry is a regular octahedron for all values of ρ_0. For small values of this parameter, the only kind of saddle on the surface $\mathcal{V}(\mathbf{R})$ occurs at the trigonal prism geometry, the result of two triangular faces of the octahedron twisting in opposite senses until they come into registration. For small values of ρ_0, the one negative force constant of the trigonal prism corresponds to this twisting of the triangular faces, and from this saddle configuration, the twist motion returns the system to its stable octahedral form. However, at a critical value of $\rho_0 = 2.1$, the force constant for slewing the trigonal prism becomes negative, destabilizing the sliding of the triangular faces away from each other and making the system into a capped, square-based pyramid (the cap being on one of the triangular faces of course). For $\rho_0 > 2.1$, the slewed structures have lower energies than the trigonal prisms and are in fact the lowest-energy saddles between the stable octahedra, which differ only by permutations of the atoms. For $\rho_0 > 4.1$, a new locally-stable structure appears, a distorted octahedron which can be pictured as an incomplete pentagonal bipyramid, in which one of the equatorial atoms has been removed. This

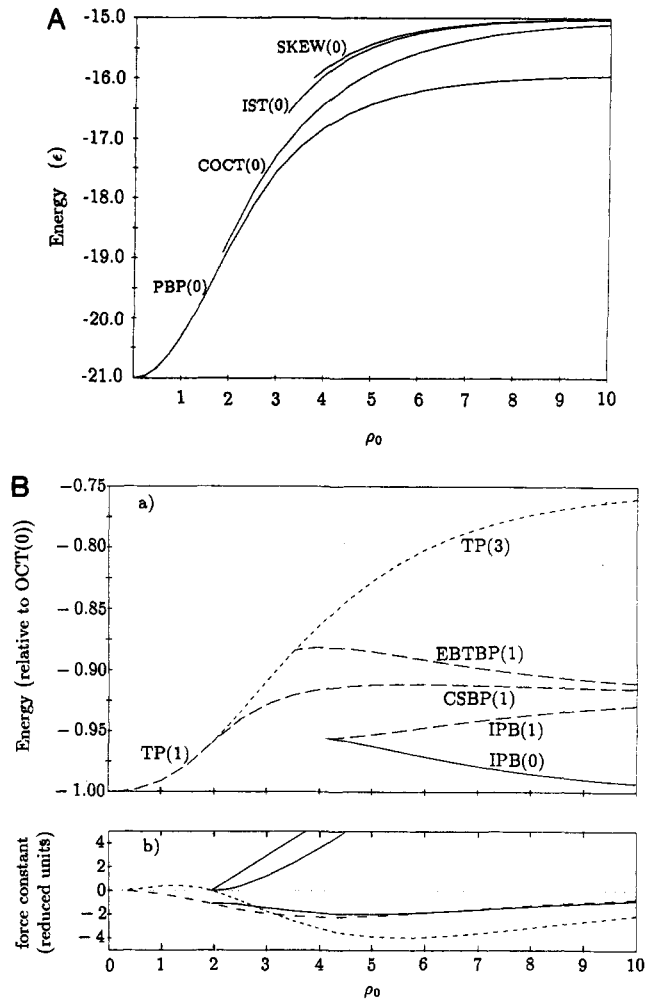

Figure 2. Behavior of (A) the minima of the "Morse" cluster M_7 as functions of the range parameter $\rho_0 = \beta R_0$ of the pairwise potential $V(\rho-\rho_0)$ and (B) the minima and saddles of the six-particle system, M_6. In (A), the energies are all in terms of the total dissociation energy; in (B), the energies are in units of the total binding energy of the most stable form, the octahedron, for each value of ρ_0. The larger ρ_0 is, the shorter is the range of the pairwise interaction; for each of the minima above the lowest, there is a value of ρ_0 below which that minimum does not exist (based on the work of Braier, Berry, and Wales[68]). In the center panel, solid curves represent minima and dashed curves represent saddles. The lower panel shows the variation of the lowest normal-mode force constants as ρ_0 varies, for the trigonal prism geometry (dashed lines) and the capped square-based prism (solid lines) to which the trigonal prism distorts at the value of ρ_0 at which the slewing mode of the trigonal prism becomes unstable.

structure has a higher energy than the regular octahedron for all values of ρ_0 (see Figure 2B).

It was thought for some time that no reaction path, i.e., no minimum-energy path between two minima, could cross a saddle of rank higher than 1[73] and that if any saddles of higher rank were to appear on the potential, there would always be a saddle of lower rank at lower energy for the reaction path to follow. The theorem on which this inference is based is correct, but its hypotheses, specifically the hypothesis that the second derivatives of the potential exist and are continuous *at the saddle point*, need not apply to all physically significant systems. Counterexamples can be constructed, the most realistic of which is the triatomic molecule with an equilateral ground state and a linear geometry at a saddle, where the doubly-degenerate bend has two equal, negative force constants.[74] Hence, it is in fact possible for reaction paths to cross saddles of rank higher than 1 and for transition states to have degenerate unstable motions, contrary to the McIver–Stanton rule on this topic.[75]

The Links to Dynamics: Rearrangements and Phase Changes

From the shapes of their potential surfaces come all dynamics of molecules and clusters. Yet the science of making this connection is just emerging; we do not yet even have a powerful set of diagnostic tools to express this connection, much less a large base of information on which to build our generalizations and intuitions. Clusters have played a stimulating part in bringing us to look at this problem, both because they have such rich, complicated potential surfaces and because as the study of clusters has grown, so has our capability to explore both structures and dynamics of these systems.

We can consider two levels of diagnosis: a more traditional approach in this section and another, somewhat less conventional, in the next. Here, we consider some of what we have learned about isomerizations, rearrangements, and phaselike behavior and how they are related to the shapes of potentials and the corresponding densities of states.

That clusters may exhibit phaselike forms—solidlike, soft-solid-like, or liquidlike—is fairly well established from theory and simulation,[76,77] although there is not yet a large body of experimental support for the phenomenon.[78-81] Moreover, clusters of many kinds and sizes, but by no means all kinds or sizes, can be expected to exhibit dynamic coexistence of two "phases" in thermodynamic equilibrium, much like chemical species in a solution in thermodynamic equilibrium. It should be mentioned here that this discussion concerns itself primarily with the thermodynamic aspects of phaselike forms of clusters, not with the kinetic aspects such as nucleation and rates of growth of phaselike forms.

For example, in an ensemble of clusters of a single composition and size such as Ar_{13}, Ar_{19}, or $(KCl)_5$, we can expect to find a stable, equilibrated ratio of solidlike and liquidlike clusters, like the stable ratio we expect to see of chemical isomers when they are in equilibrium. In restricted ranges of energies or temperatures too low to allow them to become liquidlike, clusters of six argon atoms,[82,83] six metal atoms,[84] or four KCl molecules[30] are expected on the basis of simulations to display equilibria between near-rigid, solidlike forms and nonrigid, soft-solid-like but not liquidlike forms. This kind of equilibrium entails a dynamic condition, namely, that the system spends long enough intervals in each phaselike form to develop equilibrated, observable properties characteristic of phase. If the intervals are too short, then the observer sees only averaged properties, not properties identifiable with a "phase". However, simulations have given strong indications that many kinds of clusters can be expected to satisfy this dynamic constraint and remain for tens of picoseconds to many nanoseconds in identifiable phaselike forms.

A variety of diagnostic tools have emerged for distinguishing specific phases.[76] These include the mean-square displacement in time of atoms or molecules from their initial sites; the pair distribution function; the angular distribution function;[85] the root-mean-square fractional variation of nearest-neighbor distances (the Lindemann criterion[86,87]); the velocity autocorrelation function and its Fourier transform, the power spectrum of vibrational motion, the distribution function of short-time average vibrational temperatures and the corresponding cumulative distribution; the caloric curve, i.e., the curve of mean temperature vs energy from constant-energy simulations or the curve of mean total energy or of mean potential energy vs temperature from constant-temperature simulations; and the "permutation index", a tool to distinguish soft solids from liquids, depending on whether identical atoms can eventually permute themselves among different sites.[30] Here, we shall concentrate on one of these, the distribution of short-time average temperatures.

Vibrational temperatures establish themselves quickly in classically-simulated clusters of more than three or four atoms, even when the energy or mean thermal energy of the clusters is well below the zero-point energy of the corresponding quantum cluster. Hence, it is reasonable to evaluate and use vibrational temperatures for clusters by averaging the mean internal kinetic energy of the atoms, using a relatively short averaging interval. In practice, we have usually used 500-step averages, with step lengths of 10^{-14} s for the soft Lennard-Jones systems, notably the rare gas clusters, and 3×10^{-15} s for the stiffer alkali halides such as KCl. The distributions may be binned into temperature intervals[82,88,89] or simply ordered and then plotted to give the cumulative distribution, in principle the integral of the binned distribution.[58] At low temperatures or low energies, the distributions are sharp and, except for small clusters at very low temperatures, approximately Gaussian. These correspond to clusters vibrating as solids. At high temperatures (but below the range where evaporation occurs rapidly, i.e., in 10^5–10^7 time steps), the distributions are again Gaussian but considerably broader. These correspond to liquid-like or, in some cases, soft-solid or fluxional clusters.

At intermediate temperatures, for many clusters the distributions of short-term-average temperatures are bimodal. One of the peaks can be identified readily with the solidlike form and the other with the liquidlike or fluxional form. This identification follows not only from the continuity of the bimodal peaks with the peaks in the unimodal regions. Other characteristics constructed from averages within each peak separately, such as the mean-square displacement, the power spectrum, the pair distribution, and the nearest-neighbor distance fluctuation, verify the identification of the solid and the nonrigid forms. (The only caution is that fluxionality is not a sufficient condition to imply liquidlike behavior. Clusters may be fluxional within a limited range of structures, or liquidlike without allowing for all possible permutations, or even have liquid surfaces and solid cores, thereby giving values to diagnostic indices that indicate nonrigidity yet not be truly liquid.)

Bimodality in mean temperature—or any other intensive thermodynamic quantity—is therefore a signature of coexisting forms of a cluster. If bimodality appears from a molecular dynamics simulation, it is a consequence of the time history of a cluster; if it emerges from a Monte Carlo simulation, it can be thought of as a consequence of an ensemble average. Naturally, we expect almost all clusters, under almost all conditions, to be ergodic, so the two should give the same result. There are examples, such as argon clusters from Ar_3 to at least Ar_{55} simulated at a few kelvin, which show temperature distributions that depend on initial conditions. However, these clusters simulated at about 10 K or higher, and more strongly bound clusters simulated at correspondingly higher mean temperatures show behavior insensitive to initial conditions. Hence, we have justification for our assumption of ergodicity. (This is not to say that all simulation runs give identical average results. Real runs are rarely if ever long enough with available computers to achieve fully equilibrated averages of time distributions between phases, so the time distributions fluctuate from run to run, with changes in initial conditions.)

Clusters may exhibit phaselike forms in which the cluster surface is liquidlike and the core is solidlike, so long as the liquid wets the solid. Such surface melting was first noticed in early simulations[90,91] and was explored in more detail to reveal that the mechanism of such melting is promotion of a few particles from the surface layer to the empty layer above.[92,93] This mechanism is unlike the process responsible for homogeneous melting of clusters, so that the melted surface appears not to provide nuclei for homogeneous melting. An important consequence of this is that clusters may exhibit ensembles with *more than two coexisting phaselike forms*, notably solid, surface-melted, and homogeneously melted.[94,95] It is even possible, according to the statistical-mechanical theory that describes this coexistence, for clusters to exist with a solid shell around a liquid core.

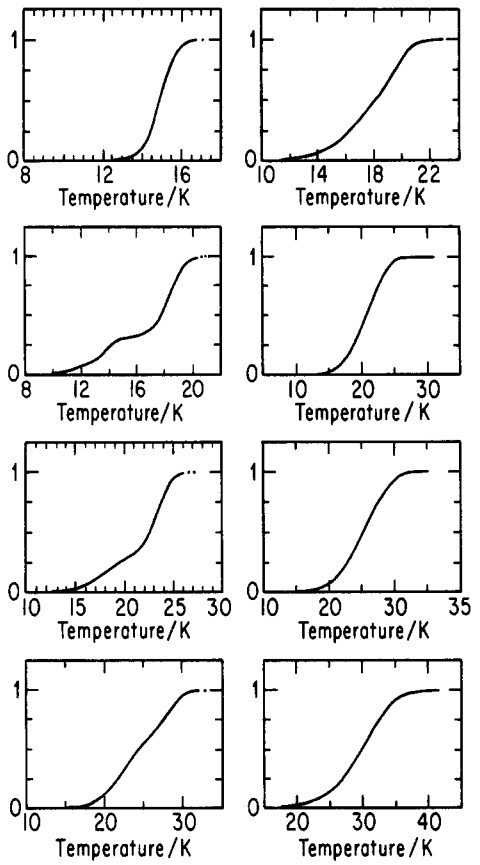

Figure 3. Cumulative distributions of mean short-range temperature for Ar_7 at several energies, from the lowest (solid range) to the highest shown (liquid range), for two values of ρ_0. For $\rho_0 = 6$, the intermediate energies show "two-step" shapes, characteristic of solid–liquid coexistence; for $\rho_0 = 4$, the cumulative distributions show only one step, implying that there is never more than a single phaselike form present (based on work of Mainz and Berry[96]).

Next, it is important to examine the relation between the shape of the multidimensional potential and the occurrence of bi- or multimodality in the distributions of short-time average temperatures. We have already seen how the shape of the potential can be altered by varying the range of the basic pairwise interaction. Now we examine what happens to the capacity of the surface to support solid and liquid phases, as a function of how simple the surface is or, more specifically, of how long is the range of the pairwise interaction.[96]

When this control is applied to clusters interacting through pairwise Morse interactions with the same well depth, interatomic distance, and curvature at the minimum of the pairwise potential as the Lennard-Jones potential for Ar–Ar, the results of constant-energy molecular dynamics simulations are essentially indistinguishable from those based on the Lennard-Jones interaction, for clusters of various sizes in the range from $N = 3$ to at least 13. When the scaled variable r is used and r_0 is the scale parameter, this corresponds to $\rho_0 = 6$. The cumulative temperature distributions for Ar_7 at several energies are shown in Figure 3. The cumulative distributions for the lowest and highest temperatures have only one point of inflection, corresponding to only one maximum in the temperature distributions themselves. However, the distributions for intermediate tempertures show distinct drops and rises in their slopes, indicating that the temperature distributions are bimodal.

If the range of the pairwise interaction is extended so that $\rho_0 = 4$, then (a) the higher minima on the surface disappear, as the results in the previous section indicated, and (b) the cumulative temperature distribution shows only one point of inflection, corresponding to a unimodal temperature distribution and to the presence at all energies of only a single phase. In short, a potential surface must have a high-lying region of secondary minima in which the system can dwell for short periods and through which the system can travel, if the system is to exhibit a liquidlike form. The potential surface for a cluster than can support liquidlike dynamics must have the form shown schematically in Figure 4, with one or more kind of deep minimum, a shallower region of many minima separated by relatively low barriers, and some kind of free energy barrier that separates the deep, solidlike gorge from the high, liquidlike rolling plain.

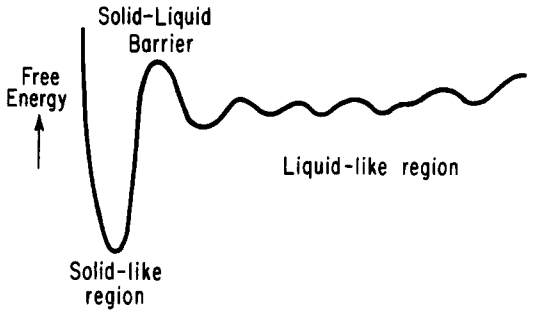

Figure 4. Schematic representation of the cross section of a potential surface capable of sustaining coexisting solidlike and liquidlike or another nonrigid forms of a cluster, in dynamic equilibrium.

The connections go further between the shape of the potential surface and the kinds of phases the cluster can exhibit. One such connection is that to the glass-forming capability of the cluster. Simulation studies have shown, particularly by quenching, that a variety of clusters have many, many high-lying minima corresponding to very disordered structures. The example that best illustrates the present topic is $(KCl)_{32}$, which has a $4 \times 4 \times 4$ rocksalt cube as its lowest-energy structure.[33,34] At about 750 K, the cluster melts, in classical simulations based on Born–Mayer pair potentials. Simulated "instantaneous" quenches from the liquid almost always bring the cluster to some high-lying, extremely disordered structure. Any ensemble of such clusters would certainly be considered amorphous or glassy by any standard diagnosis. Yet if the $(KCl)_{32}$ cluster has its energy or temperature reduced at a very high but still physically conceivable rate, e.g., 10^{12} or even 5×10^{12} K/s, corresponding to about 50 or 10 vibrational periods, respectively, the cluster finds its way to the $4 \times 4 \times 4$ cube or to some slightly defective variant. Such a victory over statistical odds must seem even more amazing than protein folding! Such effective focusing by the topography of the surface means that the many high-lying, "disordered" minima on the potential surface cannot be separated by high barriers from minima corresponding to more ordered, low-lying structures. In fact, this result suggests that perhaps the deeper a secondary minimum is on the $(KCl)_{32}$ surface, the lower is the barrier that separates it from the global minimum.

The evidence so far indicates that this interpretation is correct for $(KCl)_{32}$. Now suppose we could shorten the range of the pairwise interactions while maintaining the depth of the attractive pairwise wells between oppositely charged ions. This, like shortening the range of the Morse or inverse power potential, makes the barriers higher and generates and deepens the high-lying secondary minima on the potential surface. In practice, it is straightforward to carry out such a shortening of the range from the long-range Coulomb potential by replacing that pure R^{-1} interaction with a shielded potential, a Debye–Yukawa interaction of the form $\exp(-\kappa R)/R$. If κ is about 0.3 $bohr^{-1}$, then "realistic" cooling at about 10^{11} K/s reveals occasional disordered structures. Shortening the range still further will make the cluster less and less alkali-halide-like and more like a II–VI or III–V compound cluster. These are expected to form glasses far more readily than alkali halides.

The Links to Dynamics: Ergodicity and Chaos

In several respects, clusters are ideal systems for studying chaotic and ergodic behavior at the atomic level. They are simple enough to be tractable and complex enough to exhibit the full range of possible kinds of regular and chaotic, ergodic, and periodic behavior, are amenable to classical and quantum-mechanical treatment, and, in simulations, can be tuned to exhibit a wide range of properties. They are particularly useful for getting beyond the very simple systems of only one or two degrees of freedom that have shaped many of our ideas about chaos and ergodicity. Most probes of chaos thus far have been based on finding the positive Liapunov exponents of the system, the constants that specify the exponential rates at which neighboring pairs, triples, etc., of initially-close trajectories separate with time. The sum of the positive Liapunov exponents, shown to be equal to the Kolmogorov entropy (K-entropy), is also sometimes used to quantify the extent of chaos of a cluster.

One of the early examples in which the chaotic behavior of a system of many degrees of freedom was investigated was the study by Butera and Caravati of 100 and of 225 coupled rotors in a plane.[97] This work revealed a change in slope of the largest Liapunov exponent as a function of temperature, $\lambda_{max}(T)$, at the temperature of the Kosterlitz–Thouless transition specific to two-dimensional systems. A series of investigations have explored the Liapunov spectra of atomic fluids using, in most examples, periodic boundary conditions to simulate bulk systems rather than clusters.[98-102]

Both the chaotic and ergodic behavior of Ar_3 were studied by classical molecular dynamics,[103,104] through evaluation of the positive Liapunov exponents and K-entroy as measures of chaotic character, and the fractal dimension of the trajectory—strictly, the correlation dimension, which is a lower bound on the more familiar Hausdorff dimension—as a measure of the ergodic character of the system. This cluster is so simple that its behavior cannot be extrapolated to larger systems. Nevertheless, with its three internal degrees of vibrational freedom and six-dimensional phase space for that motion, it is a very helpful bridge between "toy" systems and systems complicated enough to justify generalizations. The equilibrium configuration of Ar_3 or any three-atom system bound by Lennard-Jones interactions is an equilateral triangle. The potential surface has saddles at each of the three linear configurations. At low (constant) energies, the classical model of this system gives rise to a short-time mean temperature distribution rather Gaussian in shape; at somewhat higher energies, high enough that the system can cross its saddles occasionally, the temperature distribution is bimodal. The low-temperature mode corresponds to systems or time intervals associated with long dwell times in the saddle regions, where the kinetic energy is low; the high-temperature peak corresponds to systems or time intervals in which the Ar_3 is like a hot solid, bouncing about high above the bottom of its deep potential well.

Throughout a low-energy range, up to just below the energy corresponding to 30 K, the K-entropy rises slowly and then more rapidly with energy. Likewise, the correlation dimension, which must in principle lie between 3 and 8, rises from essentially 3 at about 2 K to 8 at about 28 K, or -0.7ϵ/atom, in terms of the ϵ of the Lennard-Jones potential. The precise energy of the maximum depends on the particular method used to evaluate the K-entropy. At this energy, the system shows characteristics much like those we associate with melting: the power spectrum develops soft modes, the mean-square displacement rises, the nearest-neighbor distances fluctuate far more than 10% of their values, and the three-atom clusters pass fairly frequently through their linear configurations. It would be inappropriate to call this a melting transition, but it is correct to recognize that the softened Ar_3 cluster shares many properties with its larger liquid cluster counterparts.

Just above -0.7ϵ/atom, in the energy range in which the cluster can just pass at an easily detectable frequency through its saddles, the K-entroy and the fractal dimension both *drop*. In other words, according to these two diagnostics, when the three-atom cluster undergoes a transformation somewhat akin to melting, it becomes *less chaotic and less ergodic* than at energies just below that transition.

The measures of chaos—positive Liapunov exponents and their sum, the Kolmogorov entropy—come from taking the limits of propagations of the Jacobian over long trajectories. Nevertheless, the idea of associating the *local* character of the potential surface with a *local* contribution to chaotic character has fascinated investigators for some time.[104-108] If the step length of the molecular dynamics simulation is small enough, the Jacobian can be expressed in terms of simple constants and the matrix of second derivatives of the potential, the Hessian. The local Liapunov *functions*, the local analogues of the positive Liapunov exponents, emerge directly from the negative eigenvalues of the Hessian.[104,108] "Local" K-entropies, the sums of the local Liapunov functions, are not equal to the true K-entropies by any means; however, their energy dependence does mirror the energy dependence of the K-entropies, including the drop at energies above -0.7 e/atom. Overlays of contour maps of K^1, the local K-entropy or K-entropy evaluated over only one step, with contour maps of the potential surface reveal which parts of the surface contribute most to the integrals that become the positive Liapunov exponents;[104] two of these are shown in Figure 5.

If the Lennard-Jones potential for three identical atoms is replaced by a Morse potential with $\rho_0 = 6$, the Liapunov spectrum and the K-entropy are virtually unaffected. If ρ_0 is then reduced, so that the range of the pair interactions is extended, the behavior of the K-entropy does change. In particular, its energy dependence changes: if ρ_0 is lowered to 3, the K-entropy shows no maximum. For values of ρ_0 of 5 or larger, the K-entropy has a maximum at an energy that does not change with ρ_0. In other words, by extending the range (and also softening the potential), we make the high-energy passes of the potential surface into better generators of chaos. We can interpret this from the overlays: if the pair interactions are short-ranged, then the saddle region of the three-particle cluster is broad, flat, and naturally sustaining of the direction of most trajectories passing through it. If the pair interactions are long-ranged, then the saddle regions are more steep-sided and pinched, so that many trajectories through them involve collisions with the walls of the potential, which in turn makes the trajectory more chaotic.

The seven-particle Lennard-Jones cluster has no similar turnover in its K-entropy; instead, the K-entropy of this system increases monotonically with energy, through the coexistence region. The interpretation of this rise is that there are so many degrees of freedom that have noting to do with melting that their steadily-increasing chaotic character hides the drop in chaotic character associated with the mode or very few modes that develop negative force constants.[104]

Conclusion

It is now feasible to locate minima and saddles on multi-dimensional potential surfaces, even to dimensionalities of 150 or more.[109] The connectivities of fairly complex surfaces can also be established.[68] However, the microcanonical entropies of the various basins on the surfaces cannot yet be determined definitively.

The range of pair interactions influences the overall shape of the multidimensional potential. In general, the shorter are the ranges of the attractive pairwise interactions, the more and more important are the high-energy secondary minima on the multi-dimensional surface, and the more complicated that surface is. This is the case not only for homogeneous systems but also for binary, alkali halide-like systems in which the long-range Coulomb

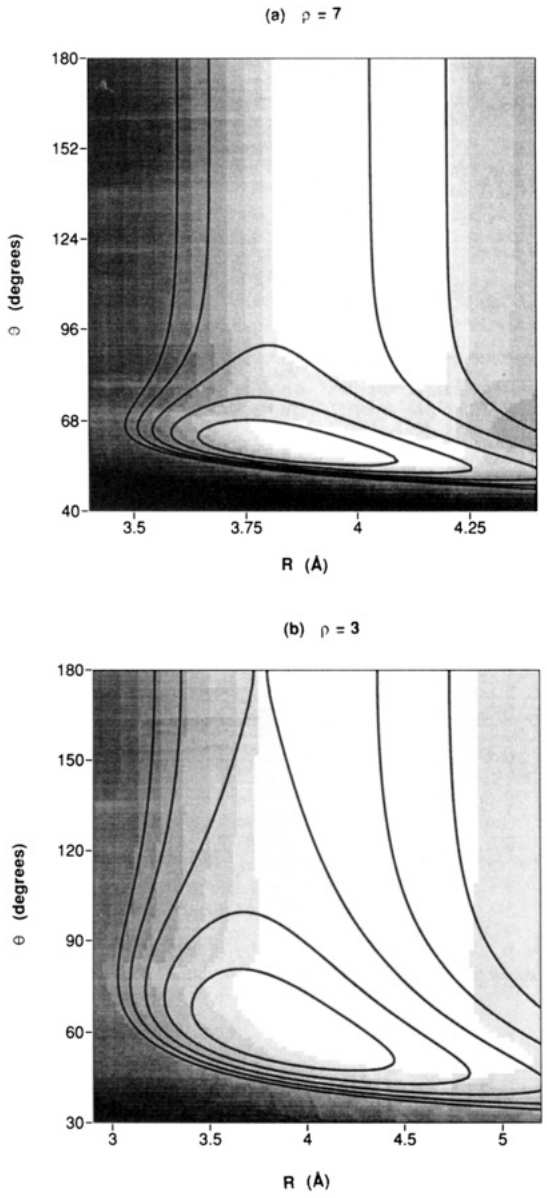

Figure 5. Overlays of the local K-entropy, K^1 (shading), and the energy contours of the potential surfaces for two three-particle clusters interacting through pairwise Morse potentials: (a) $\rho_0 = 6$; (b) $\rho_0 = 3$. These are taken from Hinde et al.[104]

potential can be converted into a shielded, Yukawa- or Debye-type potential.

In very simple systems in which each mode carries a large fraction of the total energy, such as the three-body cluster, the behavior becomes more regular and more nearly periodic-like, according to measures of the extent of chaos and ergodicity, when the energy is made high enough to allow the system to pass across saddles on its potential, particularly if the saddles are broad and flat ("Sancho Panza saddles" according to Mezey[110,111]). However, if the saddles are made steep enough, the K-entropy, which measures the degree of chaotic character, simply reaches a maximum and stays there as the energy increases, instead of dropping as it does for, for example, the three-particle Lennard-Jones cluster or presumably for Ar_3. In larger clusters this behavior is not apparent, presumably because of the number of degrees of freedom that show no such anomalous behavior and hide the behavior of the mode which turns soft when a saddle can be crossed.

This line of attack seems to be opening new kinds of insights into the connections between what we can learn about the shapes of potential surfaces and the dynamics on those surfaces. At present, it seems that the most fruitful directions will be in addressing systems of several particles, more than two or three, probably more than eight or ten—systems to which we will be unable to apply complete analyses but will have to devise combinations of statistical sampling methods and inferences based on those statistical data.

Acknowledgment. The author acknowledges the enormous contributions of his collaborators whose work is cited here. The research described here that was done at The University of Chicago was supported by grants from the National Science Foundation.

References and Notes

(1) Chasman, D.; Silbey, R. J.; Eisenberg, M. *Theor. Chim. Acta* **1991**, *79*, 175.
(2) Braier, P. A.; Berry, R. S. *J. Phys. Chem.*, in press.
(3) Beck, T.; Doll, J.; Freeman, D. *J. Chem. Phys.* **1989**, *90*, 5651–5656.
(4) Leitner, D. M.; Doll, J. D.; Whitnell, R. M. *J. Chem. Phys.* **1991**, *94*, 6644–6659.
(5) Rick, S. W.; Leitner, D. L.; Doll, J. D.; Freeman, D. L.; Frantz, D. D. *J. Chem. Phys.* **1991**, *95*, 6658–6667.
(6) Bartell, L. S.; Dulles, F. J.; Chuko, B. *J. Phys. Chem.* **1991**, *95*, 6481–6487.
(7) Bartell, L. S.; Xu, S. *J. Phys. Chem.* **1991**, *95*, 8939–8941.
(8) Bartell, L. S.; Chen, J. *J. Phys. Chem.* **1992**, *96*, 8801–8808.
(9) Aziz, R. A.; Chen, H. H. *J. Chem. Phys.* **1977**, *67*, 5719.
(10) Aziz, R. A. *Mol. Phys.* **1979**, *38*, 177.
(11) Aziz, R. A.; Slaman, M. J. *Mol. Phys.* **1986**, *58*, 679–697.
(12) Aziz, R. A. *J. Chem. Phys.* **1993**, *99*, 4518–4525.
(13) Wales, D. J. *J. Chem. Soc., Faraday Trans.* **1990**, *86*, 3505–3517.
(14) Welch, D. O.; Lazareth, O. W.; Dienes, D. J.; Hatcher, R. D. *J. Chem. Phys.* **1976**, *64*, 835–839.
(15) Welch, D. O.; Lazareth, O. W.; Dienes, G. J.; Hatcher, R. D. *J. Chem. Phys.* **1978**, *68*, 2159–2171.
(16) Hoare, M. R.; Pal, P. *Adv. Phys.* **1971**, *20*, 161–196.
(17) Hoare, M. R.; Pal, P. *Adv. Phys.* **1975**, *24*, 645.
(18) Hoare, M. R. *Adv. Chem. Phys.* **1979**, *40*, 49–135.
(19) Stillinger, F. H.; Weber, T. A. *Kinam* **1981**, *3*, 159–171.
(20) Stillinger, F. H.; Weber, T. A. *Phys. Rev. A* **1982**, *25*, 978–989.
(21) Stillinger, F. H.; Weber, T. A. *Phys. Rev. A* **1983**, *28*, 2408–2416.
(22) Mackay, A. L. *Acta Crystallogr.* **1962**, *15*, 916.
(23) Echt, O.; Kandler, O.; Leisner, T.; Miehle, W.; Recknagel, E. *J. Chem. Soc., Faraday Trans.* **1990**, *86*, 2411–2415.
(24) Martin, T. P. *J. Chem. Phys.* **1977**, *67*, 5207–5212.
(25) Martin, T. P. *J. Chem. Phys.* **1978**, *69*, 2036–2042.
(26) Martin, T. P. *J. Chem. Phys.* **1980**, *72*, 3506–3510.
(27) Martin, T. P. *Phys. Rep.* **1983**, *95*, 167–199.
(28) Diefenbach, J.; Martin, T. P. *J. Chem. Phys.* **1985**, *83*, 4585–4590.
(29) Luo, J.; Landman, U.; Jortner, J. In *Physics and Chemistry of Small Clusters*; Jena, P., Rao, B. K., Khanna, S. N., Eds.; Plenum Press: New York, 1987; p 201.
(30) Rose, J. P.; Berry, R. S. *J. Chem. Phys.* **1992**, *96*, 517–538.
(31) Heidenreich, A.; Oref, I.; Jortner, J. *J. Phys. Chem.* **1992**, *96*, 7517–7523.
(32) Heidenreich, A.; Jortner, J.; Oref, I. *J. Chem. Phys.* **1992**, *97*, 197–210.
(33) Rose, J. P.; Berry, R. S. *J. Chem. Phys.* **1993**, *98*, 3262–3274.
(34) Rose, J. P.; Berry, R. S. *J. Chem. Phys.* **1993**, *98*, 3246–3261.
(35) Martin, T. P.; Bergmann, T.; Göhlich, H.; Lange, T. *Z. Phys. B* **1991**, *19*, 25–30.
(36) Knight, W. D.; Clemenger, K.; deHeer, W. A.; Saunders, W. A.; Chou, M. Y.; Cohen, M. L. *Phys. Rev. Lett.* **1984**, *52*, 2141.
(37) Mayer, M. G.; Jensen, J. H. *Elementary Theory of Nuclear Shell Structure*; Wiley: New York, 1955.
(38) Mansikka-aho, J.; Manninen, M.; Hammarén, E. *Z. Phys. D* **1991**, *21*, 271–279.
(39) Uppenbrink, J.; Wales, D. J. *J. Chem. Soc., Faraday Trans.* **1991**, *87*, 215–222.
(40) Press, W. H.; Flannery, B. P.; Teukolsky, S. A.; Vetterling, W. T. *Numerical Recipes*; Cambridge University Press: Cambridge, 1986.
(41) Sun, J.-Q.; Ruedenberg, K. *J. Chem. Phys.* **1993**, *98*, 9707–9714.
(42) Sun, J. Q.; Ruedenberg, K. *J. Chem. Phys.* **1993**, *99*, 5257–5268.
(43) Sun, J. Q.; Ruedenberg, K. *J. Chem. Phys.* **1993**, *99*, 5269–5275.
(44) Sun, J. Q.; Ruedenberg, K. *J. Chem. Phys.* **1993**, *99*, 5276–5280.
(45) Pancik, J. *Collect. Czech. Chem. Commun.* **1975**, *40*, 1112–1118.
(46) Cerjan, C. J.; Miller, W. H. *J. Chem. Phys.* **1981**, *75*, 2800–2806.
(47) Simons, J.; Jørgenson, P.; Taylor, H.; Ozment, J. *J. Phys. Chem.* **1983**, *87*, 2745–2753.
(48) O'Neal, D.; Taylor, H.; Simons, J. *J. Phys. Chem.* **1984**, *88*, 1510–1513.
(49) Banerjee, A.; Adams, N.; Simons, J. *J. Phys. Chem.* **1985**, *89*, 52.
(50) Baker, J. *J. Comput. Chem.* **1986**, *7*, 385–395.
(51) Baker, J. *J. Comput. Chem.* **1987**, *8*, 563–574.
(52) Shida, N.; Barbara, P. F.; Almlöf, J. E. *J. Chem. Phys.* **1989**, *91*, 4061.
(53) Berry, R. S.; Davis, H. L.; Beck, T. L. *Chem. Phys. Lett.* **1988**, *147*, 13–17.

(54) Davis, H. L.; Wales, D. J.; Berry, R. S. *J. Chem. Phys.* **1990**, *92*, 4473–82.
(55) Berry, R. S. In *Mode Selective Chemistry*; Jortner, J., Pullman, A., Pullman, B., Eds.; Kluwer Academic Publishers: Amsterdam, 1991; pp 1–15.
(56) Berry, R. S. *Chem. Rev.* **1993**, *93*, 2379–2394.
(57) Stillinger, F. H.; Weber, T. A. *J. Chem. Phys.* **1984**, *80*, 4434–4437.
(58) Wales, D. J.; Berry, R. S. *J. Chem. Phys.* **1990**, *92*, 4283–4295.
(59) Cheng, H.-P.; Li, X.; Whetten, R. L.; Berry, R. S. *Phys. Rev. A* **1992**, *46*, 791–800.
(60) Zauhar, R. J.; Morgan, R. S. *J. Comput. Chem.* **1990**, *11*, 603.
(61) Saxena, S.; Bhatt, P. C. P.; Prasad, V. C. *IEEE Trans. Comput.* **1990**, *39*, 400.
(62) Edelsbrunner, H. In *Algorithms in Combinatorial Geometry*; Brauer, W., Rozenberg, G., Saloma, A., Eds.; Springer-Verlag: New York, 1987; Chapter 13.
(63) Robinson, P. J.; Holbrook, K. A. *Unimolecular Reactions*; Wiley-Interscience: London, 1972.
(64) Stillinger, F. H.; Weber, T. A. *J. Chem. Phys.* **1984**, *81*, 5095–5103.
(65) Ferrenberg, A. M.; Swendsen, R. H. *Phys. Rev. Lett.* **1989**, *63*, 1195–1198.
(66) Labastie, P.; Whetten, R. L. *Phys. Rev. Lett.* **1990**, *65*, 1567–1570.
(67) Reinhardt, W. P.; Hunter, J. E., III *J. Chem. Phys.* **1992**, *97*, 1599–1601.
(68) Braier, P. A.; Berry, R. S.; Wales, D. J. *J. Chem. Phys.* **1990**, *93*, 8745–8756.
(69) Stillinger, F. H.; Stillinger, D. K. *J. Chem. Phys.* **1990**, *93*, 6106–6107.
(70) Piela, L.; Kostrowicki, J.; Scheraga, H. A. *J. Phys. Chem.* **1989**, *93*, 3339–3346.
(71) Kostrowicki, J.; Piela, L.; Cherayil, B. J.; Scheraga, H. A. *J. Phys. Chem.* **1991**, *95*, 4113–4119.
(72) Pillardy, J.; Olszewski, K. A.; Piela, L. *J. Phys. Chem.* **1992**, *96*, 4337–4341.
(73) Murrell, J. N.; Laidler, K. J. *Trans. Faraday Soc.* **1968**, *64*, 371.
(74) Wales, D. J.; Berry, R. S. *J. Chem. Soc., Faraday Trans.* **1992**, *8*, 543–544.
(75) McIver, J. W. *Acc. Chem. Res.* **1974**, *7*, 72–77.
(76) Berry, R. S.; Beck, T. L.; Davis, H. L.; Jellinek, J. In *Evolution of Size Effects in Chemical Dynamics, Part 2*; Prigogine, I., Rice, S. A., John Wiley and Sons: New York, 1988; Vol. 70, pp 75–138.
(77) Sugano, S. *Microcluster Physics*; Springer-Verlag: Berlin, 1991; Vol. 20, p 158.
(78) Bartell, L. S.; Harsanyi, L.; Valente, E. J. *J. Phys. Chem.* **1989**, *93*, 6201–6205.
(79) Bartell, L. S.; Harsanyi, L.; Dibble, T. S.; Lennon, P. J. *J. Phys. Chem.* **1990**, *94*, 6009.
(80) Lermé, J.; Bordas, C.; Pellarin, M.; Baguenard, B.; Vialle, J. L.; Broyer, M. *Phys. Rev. B* **1993**, *48*, 12110–12122.
(81) Martin, T. P.; Näher, U.; Schaber, H.; Zimmerman, U. *J. Chem. Phys.* **1994**, *100*, 2322.
(82) Beck, T. L.; Jellinek, J.; Berry, R. S. *J. Chem. Phys.* **1987**, *87*, 545–554.
(83) Beck, T. L.; Berry, R. S. *J. Chem. Phys.* **1988**, *88*, 3910–3922.
(84) Sawada, S.; Sugano, S. *Z. Phys. D* **1989**, *12*, 189.
(85) Quirke, N.; Sheng, P. *Chem. Phys. Lett.* **1984**, *110*, 63–66.
(86) Lindemann, F. A. *Phys. Z.* **1910**, *11*, 609.
(87) Lindemann, F. A. *Engineering* **1912**, *94*, 515.
(88) Jellinek, J.; Beck, T. L.; Berry, R. S. *J. Chem. Phys.* **1986**, *84*, 2783–2794.
(89) Davis, H. L.; Jellinek, J.; Berry, R. S. *J. Chem. Phys.* **1987**, *86*, 6456–6469.
(90) Briant, C. L.; Burton, J. J. *J. Chem. Phys.* **1975**, *63*, 2045–2058.
(91) Nauchitel, V. V.; Pertsin, A. J. *Mol. Phys.* **1980**, *40*, 1341–1355.
(92) Cheng, H.-P.; Berry, R. S. In *Symposium on Clusters and Cluster-Assembled Materials*; Materials Research Society: 1991; pp 241–252.
(93) Cheng, H.-P.; Berry, R. S. *Phys. Rev. A* **1992**, *45*, 7969–7980.
(94) Kunz, R. E.; Berry, R. S. *Phys. Rev. Lett.* **1993**, *71*, 3987–3990.
(95) Kunz, R. E.; Berry, R. S. *Phys. Rev. E* **1994**, *49*, 1895–1908.
(96) Mainz, D.; Berry, R. S. Manuscript in preparation.
(97) Butera, P.; Caravati, G. *Phys. Rev. A* **1987**, *36*, 962–964.
(98) Evans, D. J.; Cohen, E. G. D.; Morriss, G. P. *Phys. Rev. A* **1990**, *42*, 5990.
(99) Hoover, W. G.; Posch, H. A.; Bestiale, S. *J. Chem. Phys.* **1987**, *87*, 6665.
(100) Posch, H. A.; Hoover, W. G. *Phys. Rev. A* **1989**, *39*, 2173.
(101) Posch, H. A.; Hoover, W. G.; Holian, B. L. *Ber. Bunsen-Ges. Phys. Chem.* **1990**, *94*, 250.
(102) Posch, H. A.; Hoover, W. G. *Phys. Rev. A* **1988**, *38*, 473.
(103) Beck, T. L.; Leitner, D. M.; Berry, R. S. *J. Chem. Phys.* **1988**, *89*, 1681–1694.
(104) Hinde, R. J.; Berry, R. S.; Wales, D. J. *J. Chem. Phys.* **1992**, *96*, 1376–1390.
(105) Brumer, P.; Duff, J. W. *J. Chem. Phys.* **1976**, *65*, 3566.
(106) Duff, J. W.; Brumer, P. *J. Chem. Phys.* **1977**, *67*, 4898.
(107) Kosloff, R.; Rice, S. A. *J. Chem. Phys.* **1981**, *74*, 1947.
(108) Wales, D. J.; Berry, R. S. *J. Phys. B* **1991**, *24*, L351–357.
(109) Wales, D. J. *Chem. Phys. Lett.* **1990**, *166*, 419–424.
(110) Mezey, P. G.; Peterson, M. R.; Csizmadia, I. G. *Can. J. Chem.* **1977**, *55*, 2941–2945.
(111) Mezey, P. G. *Potential Energy Hypersurfaces, Studies in Physical and Theoretical Chemistry*; Elsevier: Amsterdam, 1987; Vol. 53.